Acta Biomaterialia 123 (2021) 346–353

Contents lists available at ScienceDirect

Acta Biomaterialia

journal homepage: www.elsevier.com/locate/actbio

Full length article

Nanoparticles for delivery of agents to fetal lungs

Sarah J. Ullrich[a,*], Mollie Freedman-Weiss[a,*], Samantha Ahle[a], Hanna K. Mandl[b], Alexandra S. Piotrowski-Daspit[b], Katherine Roberts[a], Nicholas Yung[a], Nathan Maassel[a], Tory Bauer-Pisani[a], Adele S. Ricciardi[a,b], Marie E. Egan[c], Peter M. Glazer[d,e], W. Mark Saltzman[b,f,g], David H. Stitelman[a]

[a] Department of Surgery, Yale University, 330 Cedar Street, FMB 107, New Haven, CT, 06510, USA
[b] Department of Biomedical Engineering, Yale University, New Haven, CT, 06511, USA
[c] Division of Pulmonary Allergy Immunology Sleep Medicine, Department of Pediatrics, School of Medicine, Yale University, New Haven, Connecticut, USA
[d] Department of Therapeutic Radiology, Yale University, New Haven, CT, 06520, USA
[e] Department of Genetics, Yale University, New Haven, CT, 06520, USA
[f] Department of Chemical & Environmental Engineering, Yale University, New Haven, CT, 06511, USA
[g] Department of Physiology, Yale University, New Haven, CT, 06511, USA

ARTICLE INFO

Article history:
Received 13 October 2020
Revised 1 January 2021
Accepted 18 January 2021
Available online 21 January 2021

Keywords:
Fetal therapy
Lung targeting
Biodegradable nanoparticles
Biodistribution

ABSTRACT

Fetal treatment of congenital lung disease, such as cystic fibrosis, surfactant protein syndromes, and congenital diaphragmatic hernia, has been made possible by improvements in prenatal diagnostic and interventional technology. Delivery of therapeutic agents to fetal lungs in nanoparticles improves cellular uptake. The efficacy and safety of nanoparticle-based fetal lung therapy depends on targeting of necessary cell populations. This study aimed to determine the relative distribution of nanoparticles of a variety of compositions and sizes in the lungs of fetal mice delivered through intravenous and intra-amniotic routes. Intravenous delivery of particles was more effective than intra-amniotic delivery for epithelial, endothelial and hematopoietic cells in the fetal lung. The most effective targeting of lung tissue was with 250nm Poly-Amine-co-Ester (PACE) particles accumulating in 50% and 44% of epithelial and endothelial cells. This study demonstrated that route of delivery and particle composition impacts relative cellular uptake in fetal lung, which will inform future studies in particle-based fetal therapy.

Statement of significance

Nanoparticle-based fetal lung therapy can be used to treat congenital lung diseases *in utero*, before permanent damage to the lungs occur after birth. Optimizing nanoparticle delivery to target specific cell populations can allow for more efficacious delivery of therapeutic agents. This study determined the relative distribution of nanoparticles of a variety of compositions and sizes delivered *in utero* through intravenous and intra-amniotic routes. Intravenous delivery of particles was more effective than intra-amniotic delivery for targeting epithelial, endothelial and hematopoietic cells in the fetal lung. This will inform future studies in particle-based fetal therapy for congenital lung diseases.

1. Introduction

Diagnosing hereditary and congenital lung disorders *in-utero* is now possible due to advances in prenatal screening such as non-invasive genetic testing and high-resolution ultrasound. Despite the availability of prenatal detection, there are no current *in-utero* treatment options for such lung disorders. Conditions such as cystic fibrosis (CF), surfactant protein syndromes, and congenital diaphragmatic hernia (CDH) remain significant sources of irreversible neonatal and pediatric morbidity and mortality [1–4]. Advances in gene therapy have led to increased interest in strategies such as gene addition and CRISPR/Cas-based gene editing approaches to treat monogenic lung disorders such as CF, alpha-1 antitrypsin deficiency, and surfactant protein deficiencies [5,6]. Furthermore, ad-

* Corresponding author.
E-mail address: sarah.ullrich@yale.edu (S.J. Ullrich).

https://doi.org/10.1016/j.actbio.2021.01.024
1742-7061/

vances in the understanding of epigenetics and the role of microRNAs (miRNAs) as disease mediators in conditions such as CDH and bronchopulmonary dysplasia has led to the investigation of miRNAs as therapeutic agents to promote lung growth in utero [7–10].

In-utero treatment via delivery of gene vectors, nucleic acids, proteins, or other therapeutic agents is of clinical interest due to favorable features of a fetal host. Most encouraging regarding fetal treatment is the ability to alter and improve dysfunctional development and halt irreversible damage that occurs before birth. In contrast to post-natal gene therapy, fetal gene therapy also allows for the induction of immune tolerance to transgene products. Additionally, the small size of the fetus allows for the delivery of high relative doses using minimal reagents [11,12].

Viral vectors have been studied in animal models for fetal therapy, however their use is limited by safety concerns related to adverse host and maternal immune responses and high rates of fetal demise [13]. Polymeric nanoparticles (NPs) are promising vehicles for the controlled delivery of a wide variety of therapeutic agents since they can be non-toxic and have low side effects [14–17]. We have previously demonstrated that intravenous (IV) and intra-amniotic (IA) administration of degradable polymer NPs containing peptide nucleic acids (PNAs) for gene editing is safe without any adverse effects on survival, growth patterns or levels of pro-inflammatory cytokines; and that fetal delivery resulted in sustained phenotypic correction of a mouse model of human β-thalassemia [18]. In these studies, we have also observed delivery of the NPs to fetal lung tissue, suggesting an avenue by which therapeutics can be effectively delivered to the lung for congenital pulmonary diseases.

The fate of NPs in adult animals can be modulated by altering factors such as their route of administration, size, charge, and hydrophobicity [19]. Poly(lactic-co-glycolic) acid (PLGA) NPs have been widely used to deliver therapeutic agents [20]. The size of PLGA NPs can be altered, which has been demonstrated to affect biodistribution in adult mice [21]. Another family of polymeric delivery vehicles composed of poly(amine-co-esters) (PACEs) are promising particularly for the delivery of nucleic acids, as they are cationic, but have low toxicity, and can load nucleic acids at higher efficiencies than NPs made of PLGA or other materials [22,23]. Certain surface modifications to NPs, such as with poly(ethylene glycol) (PEG), increase their hydrophilicity– reducing their interaction with serum proteins and increasing the time spent in circulation [24].

The effects of such parameters on tissue-specific accumulation of NPs have been demonstrated in adult mice after IV injection, however there have been no studies investigating how these parameters affect the biodistribution of NPs in fetal lung after *in-utero* IV and IA injection [21,25–27]. In this study we sought to determine the influence of some of these relevant features of NP design on their ability to reach specific cell populations in fetal lung and thus determine the NP type and delivery method for targeting the fetal lung.

2. Methods

2.1. Materials

Poly(D,L-lactide-co-glycolide); (Mw= 5-10 kDa, LA:GA = 50:50) and poly(D,L-lactide)-b-poly(ethylene glycol)-carboxylic acid (PLA-PEG) (Mw PLA = 16 kDa, Mw PEG = 5 kDa) were purchased from PolySciTech (West Lafayette, IN). Acetonitrile (ACN) and dimethyl sulfoxide (DMSO) were purchased from J.T. Baker (Phillipsburg, NJ). Poly(vinyl alcohol) (PVA) was purchased from Sigma-Aldrich (St. Louis, MO). For PACE NPs, 15-pentadecalactone (PDL, 98%), diethyl sebacate (DES, 98%), sebacic acid (SA, 98%), N-methyldiethanolamine (MDEA, 99+%), polyethylene glycol (PEG, 5000 MW), and diphenyl ether (99%), immobilized Candida Antarctica lipase B (CALB) supported on Novozym 435, chloroform (HPLC grade), chloroform-d (NMR grade), dichloromethane (HPLC grade, 99+%), hexanes (HPLC grade, 97+%), and methanol (98%) were purchased from Sigma Aldrich (St. Louis, MO) and used as received. The 3,3'-dioctadecyloxacarbocyanine perchlorate (DiO) dye was obtained from Biotium (Fremont, CA).

2.2. Nanoparticle preparation

PLGA and PLA-PEG NPs containing DiO dye as a fluorescent tracer were formulated using the NanoAssemblr Benchtop instrument (Precision Nanosystems Inc.), as previously reported [21]. To formulate 150 nm and 250 nm PLGA NPs, 20 mg and 25 mg of polymer was each dissolved overnight in 1 mL of ACN, respectively. To prepare 150 nm PLA-PEG NPs, 30 mg of polymer was dissolved overnight in 1 mL of 75:25 DMSO:ACN [28]. DiO dye was encapsulated in the NPs by adding 0.5% (wt/wt) of 10 mg/mL DiO in DMSO to the polymer solution.

For PLGA NPs, the aqueous phase consisted of 1 mL of 2% PVA and the NanoAssemblr flow rate was set at 8 mL/min. For PLA-PEG NPs, the aqueous phase consisted of 1 mL of water and the flow rate ran at 2 mL/min. To synthesize each batch of NPs, the organic polymer/dye and aqueous phases were simultaneously injected into the NanoAssemblr ports. NPs were collected in DI water by centrifugation using Amicon Ultra-15 filters (100 K cutoff) at 4,000 g at 4°C for 45 min three times. After the final wash, trehalose was added as a cryoprotectant at 100% (wt/wt) to PLGA NPs before lyophilization. PLA-PEG NPs were resuspended in 1x PBS and flash-frozen until use.

PACE synthesis and NP formulation have been described in detail previously [23]. Here, we used PACE and PACE-PEG with 60% PDL content. PACE NPs were formulated using a modified oil-in-water (o/w) single-emulsion solvent evaporation technique, as described previously [22,23]. Polymers were stored in airtight, sealed vessels in a desiccator box at -80°C until needed. NPs were evaluated by electron microscopy and dynamic light scattering. Characteristics of NPs are displayed in Table 1.

2.3. In vivo NP administration

All procedures and experiments were performed in accordance with the guidelines and policies of the Yale Animal Resource Center (YARC) and approved by the Yale University Institutional Animal Care and Use Committee (IACUC). Female C57BL/6 mice were obtained from Charles River Laboratories. Time dated pregnant mice between 15–17 days post conception were anesthetized with inhaled isoflurane (2% vol/vol for induction and maintenance). Analgesia was provided with subcutaneous injection of either or both of the following analgesics: 0.1mL Buprenorphine HCl (0.015 mg/mL) and 0.1 mL Meloxicam (0.1 mg/mL). The gravid uterus was exposed through a midline laparotomy incision. Fluorescent NPs were resuspended by vortex and water bath sonication in 1 × dPBS to a concentration of 12 mg/mL. IV injections were performed at gestational day e15. A volume of 15 μl of 12 mg/mL NPs (~300 mg/kg) suspension was drawn up into a glass micropipette (tip diameter ~50 μm) and injected into the vitelline vein of each fetus using a pneumatic microinjector (Narishige; Japan). IA injections were performed at e16 (310 mg/kg) and e17 (270 mg/kg), as this marks the onset of regular fetal respirations [29]. A volume of 20 μl of 12 mg/ml NP suspension was injected directly into the amniotic cavity, in the space between the forelimbs and hindlimbs of each fetus. In order to enhance respiratory drive, NPs were resuspended in theophylline (0.8 mg/mL) in select experiments [30,31]. Pregnant mice were sacrificed at 3 hours and 24

Table 1
Diameter, PDI and Zeta Potential of NP formulations.

NP Formulation	Diameter (nm)	PDI (polydispersity index)	Zeta Potential
PLGA 150	160 + 4.8	0.11 ± 0.021	-20[a]
PLGA 250	250 ± 2.5	0.16 ± 0.015	-20[a]
PLA – PEG 150	150 ± 1.7	0.31 ± 0.027	-7 ± 1[b]
PACE 250	260 ± 3.9	0.14 ± 0.019	±31 ± 0.5
PACE – PEG 150	190 ± 1.2	0.24 ± 0.017	±31 ± 0.3

[a] Estimated from previous measured of nearly identical materials[21]
[b] Estimated from previous measured of nearly identical materials[56]

hours post-injection and fetuses were delivered by cesarean section. The three-hour time point was chosen because previous in vitro experiments have demonstrated that for the polymer types examined, the majority of its NP contents are released within that time frame. [18,23] All fetuses included in the analysis were confirmed to alive at the time of delivery by the present of fetal movement.

2.4. Fluorescence microscopy

Fetuses were fixed overnight in 4% paraformaldehyde (Electron Microscopy Sciences; Hartfield, PA) at room temperature. The tissues were next dehydrated in 20% sucrose for 24 hours and embedded in Tissue-Tek Optimal Cutting Temperature (OCT) Compound (Sakura, Torrance, CA). Frozen 15 μm-thick sections were mounted on glass slides using VECTASHIELD Hardset Antifade Mounting Medium with DAPI (Vector Laboratories, Burlingame, California). Confocal imaging of the frozen sections was performed on a Zeiss Axio Observer Z1 microscope (Oberkochen, Germany). All images were processed using Zeiss Zen Pro software (Oberkochen, Germany). Only fetal lungs were assessed.

2.5. Flow cytometry

Individual fetal lungs were harvested and homogenized in 2% fetal bovine serum (FBS) in PBS using a 70 μm cell strainer. The resulting single cell suspension was pelleted and resuspended in 2% FBS in PBS and incubated with a 1:1000 dilution of FcR Blocking reagent (Cat # 130-059-901, Miltenyi Biotec Inc., Auburn, CA) for 30 minutes. Fetal lungs were subsequently stained for CD326 (EpCAM)-Super Bright 436 (Cat # 62-5791-82, Invitrogen, Carlsbad, CA), CD31(PECAM-1)-APC (Cat# 17-0311-82, Invitrogen, Carlsbad, CA), and CD45R(B220)-PE-Vio770 (Cat# 130-102-817, Miltenyi Biotec Inc., Auburn, CA). Aliquots of lung cells were also stained using SYTOX Orange Dead Cell Stain (Cat# S3486, Invitrogen, Carlsbad, CA). Cells were immediately analyzed by flow cytometry (BD LSRII 5-UV) and cell analysis was performed using FlowJo (Version 10.6.1, Ashland, OR). Cell populations were defined as follows: epithelial, CD326+CD31−CD45−; endothelial, CD326−CD31+CD45-; hematopoietic lineage, CD31−CD45+ as previously described (Supplementary Figure 1) [32].

2.6. Statistical analysis

The mean percentage of cells with NPs for each cell type with the associated standard deviation (± s.d.) were calculated. NP delivery routes were compared using one-way ANOVA, followed by Dunnett's post-hoc test for multiple comparisons or an unpaired student's t-test where appropriate. Sidak correction was used to correct for multiple comparisons to decrease the chance of a Type I statistical error. Statistical analyses were carried out using GraphPad Prism (Version 8.0, San Diego, CA) . A p-value of less than 0.05 was considered statistically significant. All reported n values represent individual fetuses. Minimum samples sizes were determined using G*Power software (Version 3.1, Bonn, Germany) with the goal of detecting a very large effect size.

We first sought to compare different methods NP delivery to fetal lung at different gestational ages using 250nm PLGA NPs: we compared IV injection at e15 (n=5) and IA injection at e16 (n=9) and e17 (n=9). We then sought to compare the effect of size, PEGylation and surface charge on NP delivery to fetal lung after e15 IV injection by comparing different sized PLGA (150nm, n=7, 250nm n=5), PLA-PEG (n=3), PACE (n=5) and PACE-PEG (n=4) NPs. We then examined the effects of size and PEGylation on delivery after e16 IA injection (150nm PLGA n =3, 250nm PLGA n=9, PLA-PEG n=3) and e17 IA injection (150nm PLGA n =8, 250nm PLGA n=9, PLA-PEG n=4). Finally, we sought to optimize IA injection conditions at e16 and e17 by comparing fetuses injected under standard experimental conditions (with narcotic analgesia and no theophylline, e16 n=9, e17 n=9) and those injected under optimized conditions (no narcotic analgesia, theophylline added, e16 n=11, e17 n=9).

3. Results

3.1. IV injection delivers NPs to fetal lung more efficiently than IA injection

We compared the efficiency of dye (DiO)-loaded 250nm PLGA NP delivery to fetal lung after intravenous (IV) injection at e15 via the vitelline vein to intra-amniotic (IA) injection at e16 and e17. The vitelline vein (accessed for IV injections) involutes after e15, which is at the end of the pseudoglandular stage of fetal lung development, making IV injection impractical after this time point. In humans, the pseudoglandular stage ends at approximately 17 weeks of gestation, where therapeutic delivery of agents to the fetus is possible. Fluorescent NPs were delivered by IA injections at e16 and e17, based on our prior results demonstrating no uptake in the lung before e16 as there is minimal breathing in the fetal mouse before this time [18]. Flow cytometry (Supplementary Figure 1) was used to determine the biodistribution of different NPs to epithelial, endothelial, and hematopoietic lineage cells (Fig. 1A, Supplementary Table 1). For all statistical analyses, e16 IV injections were used as controls (Fig. 1A). Flow cytometric analysis demonstrated that e15 IV injection delivered PLGA NPs most efficiently to all cell types; NP uptake was observed in 8%(P=<0.0001) of all cells, 26%(P<0.0001) of epithelial cells, 11%(P<0.0001) of endothelial cells and 38% (P=0.0003) of hematopoietic lineage cells. Lower uptake was noted in lung cells following e16 IA injection, with NPs in 0.5% of all cells, 0.6% of epithelial cells, endothelial cells (0.2%) and hematopoietic cells (2%). Low but improved uptake was noted in lung cells following e17 IA injection with 3%(P=0.0511) of all cells noted to have NPs in epithelial cells (7%, P=0.0214) endothelial cells (2%, P=0.0412) and hematopoietic cells (15%, P=0.0146).

Delivery of NPs to lung tissue was further assessed qualitatively via confocal microscopy (Fig. 1 B,C,D). By microscopy, IV injection (Fig. 1B) resulted in diffuse uptake in lung tissue while IA injection resulted in NP deposition in the luminal surface of the

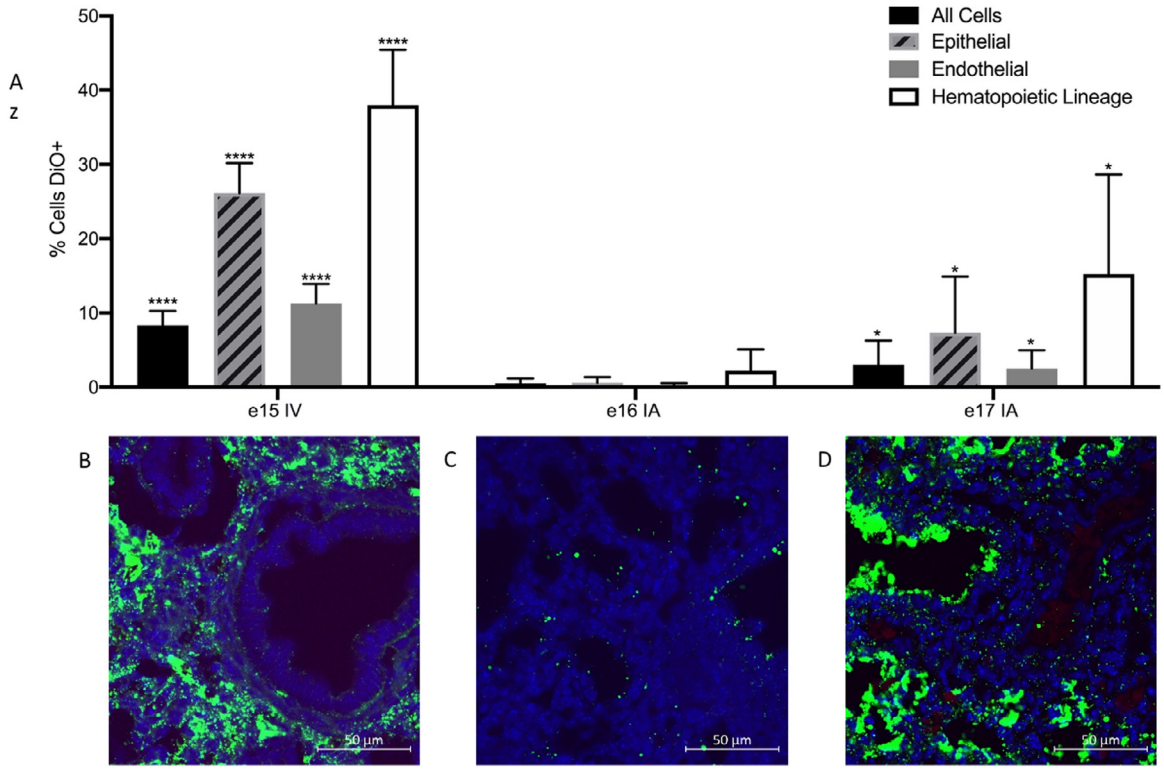

Fig. 1. A) IV injection results in greater fetal lung uptake of PLGA NPs than IA injection. Bar graph showing the percent of DiO positive epithelial, endothelial and hematopoietic lineage cells after e15 IV, e16 IA and e17 IA injection based on flow cytometry, control e16 IA, *, $p<0.05$, ****, $p< 0.0001$ (1-way ANOVA. Error bars represent S.D.) n=5-9 B-D) Immunofluorescence images (40x) of fetal lungs after 250 nm PLGA NP delivery via B) e15 IV injection, C) e16 IA injection and D) e17 IA injection. Scale bar on images represents 50μm.

lung (Fig. 1C&D). There was no fluorescence observed in uninjected lungs at e15, 16 or 17 (Supplementary Figure 2).

3.2. NP size, polymer type and surface modification affect NP delivery to the lung

To determine the effect of size, PEGylation and surface charge on NP delivery to fetal lung, DiO-loaded PLGA (150nm and 250nm), PLA-PEG (150nm), PACE (250nm) and PACE-PEG (150nm). NPs were delivered via IV injection to fetal mice at e15. Flow cytometry was used to determine whether there was a difference in the biodistribution of different NP types to total cells (Fig. 2A) (Supplementary Tables 2-4). These findings were also assessed qualitatively via confocal microscopy (Fig. 2B-F).

Two different sizes of PLGA (150nm and 250nm) were compared (Supplementary Table 2). For this analysis 150nm PLGA 150 was considered a control. Larger size NPs were delivered to less cells overall (8% vs 28%, *P*=0.0101, Fig. 3A), less epithelial cells (26% vs 40%, *P*=0.0480, Fig. 3B), less endothelial cells (11% vs 22%, *P*=0.0177, Fig. 3C) and more hematopoietic lineage cells (38% vs 28%, *P*=0.0303, Fig. 3D).

The biodistribution of PEGylated particles was investigated using 150nm PLA-PEG and 150nm PACE-PEG (Supplementary Table 3). For this analysis 150nm PLGA 150 was considered a control. There was no significant difference in NP delivery of either PEGylated particle to the total lung (Fig. 3E). PLA-PEG was delivered to less epithelial cells (40% vs 19%, *P*=0.0448, Fig. 3F). Endothelial cells had increased uptake of both particle types: PLA-PEG (37% vs 22%, *P*=0.0041, Fig. 3G) and PACE-PEG (35% vs 22%, *P*=0.0072, Fig. 3G). There was no significant difference in PEGylated NP uptake in hematopoietic lineage cells (Fig. 3H).

Differences in the biodistribution of two particles with different surface charges (250nm PLGA and 250nm PACE) were also compared after IV injection at e15 (Supplementary Table 4). For this analysis 150nm PLGA 150 was considered a control. PACE was delivered more efficiently to all cells (37% vs 8%, *P*=0.0079, Fig. 3I), epithelial cells (50% vs 26, *P*=0.0079, Fig. 3J) and endothelial cells (44% vs 11%, *P*=0.0177, Fig. 3K). There was no statistically difference in NP delivery to hematopoietic cells.

To determine the which polymer size and type was delivered most efficiently to the fetal lung after IA injection, DiO-loaded PLGA and PLA-PEG NPs were delivered via IA injection at e16 (150nm PLGA, 250nm PLGA, 150nm PLA-PEG) and e17 (150nm PLGA, 250nm PLGA, PLA-PEG). At each gestational day, fetuses injected with 150nm PLGA particles were considered controls. For e17 IA injection, 250nm PLGA NPs were delivered more efficiently to endothelial cells (2% vs 0.3%, *P*=0.0301, Fig. 4A and B). No other statistically significant differences in NP delivery were noted.

3.3. Theophylline and narcotic exposure do not change the efficiency of IA injection

Given the low delivery efficiency of NP delivery following IA injections, we sought to optimize fetal respirations to improve NP delivery. IA injections at e16 and e17 were performed using 250 nm PLGA NPs reconstituted with theophylline, which has been demonstrated to improve the delivery of other vehicles to fetal lung after IA injection [31]. Analgesia was provided with meloxicam only without the addition of opioid which could act as a respiratory suppressant. Thus there were two experimental groups at each gestational age – fetuses injected under standard experimental conditions (with narcotic analgesia and no theophylline) and those injected under optimized conditions (no narcotic analgesia, theophylline added). At each gestational day, fetuses injected under standard conditions were considered controls for statistical analysis. NP delivery was quantified as above using flow cytome-

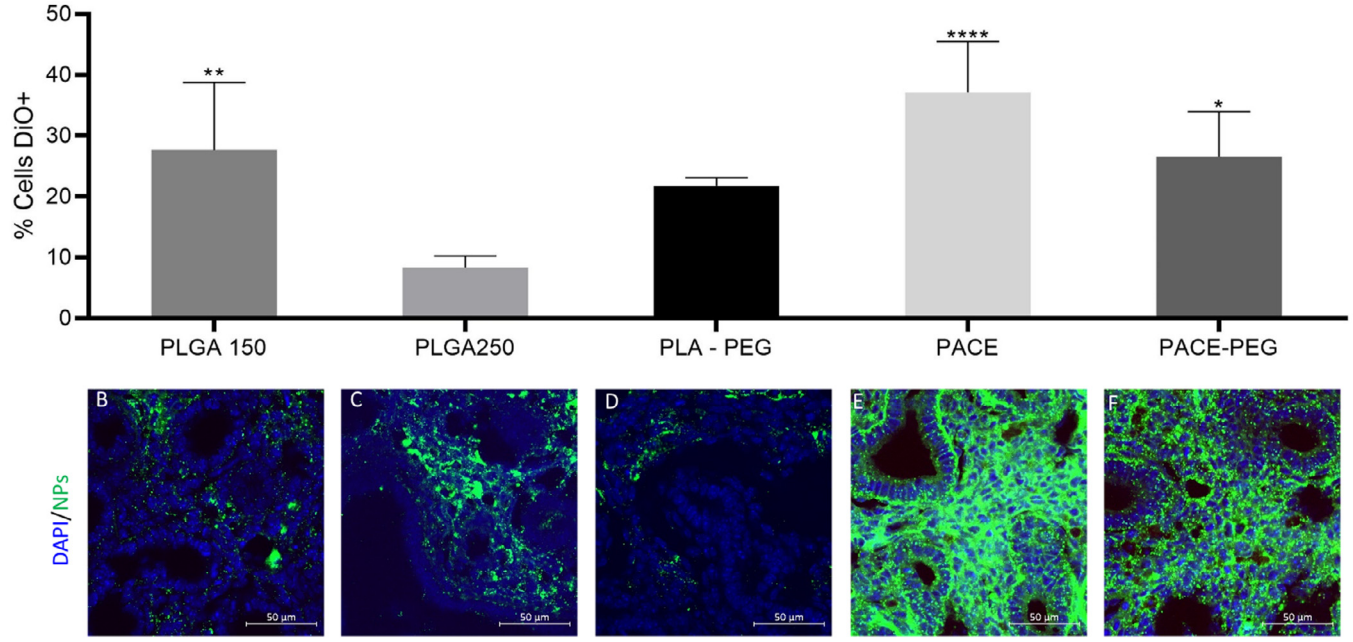

Fig. 2. Polymer type, size and surface modification impact NP delivery to lung after e15 IV injection. A) Bar graph showing the percent of DiO positive total cells after e15 IV injection. 250nm NPs were considered controls. *, p< 0.05, ***, p<0.001,****, p< 0.0001(1-way ANOVA. Error bars represent S.D.) n=3-9B) Immunofluorescence images (40x) of fetal lungs after e15 IV injection of 150 nm PLGA NPs C) 250 nm PLGA NPs D) 150 nm PLA-PEG NPs E) 250 nm PACE NPs F) 150 nm PACE-PEG NPs. Scale bar on images represents 50μm.

try. Compared to standard injections with 250 nm PLGA NPs under standard conditions, the addition of theophylline and removal of maternal narcotic exposure did not improve IA NP delivery at e16 for any cell types (Fig. 4C). Addition of theophylline and withholding narcotics during e17 injection did not improve uptake in epithelial or endothelial cells, however it did lead to an improvement in delivery of NPs to hematopoietic cells (15% to 34%, p=0.0325) (Fig. 4D).

4. Discussion

Fetal NP-mediated delivery of therapeutic agents to the developing lung is a promising strategy for the treatment of congenital lung disease. Gene editing technologies, such as PNA and CRISPR/Cas9, are potential avenues for the treatment of monogenic pulmonary disease, such as CF and surfactant protein deficiencies [6,33]. Furthermore, due to their pleotropic nature and ability to alter entire biologic pathways, miRNA therapeutics have emerged as a promising treatment for conditions mediated largely by epigenetics, such as pulmonary hypoplasia associated with CDH [7,8,34]. Polymeric NPs are safe and promising vehicles for the delivery of such therapeutics. The ability to optimize NPs and target specific tissues makes NP-mediated delivery even more promising [35].

IA injection has been described previously for the delivery of viral vectors in studies examining the in-utero treatment of cystic fibrosis and inherited surfactant protein syndromes [6,36]. In addition to being technically easier, in theory IA delivery has the added advantage of more specific targeting of fetal lung epithelial cells, which are of interest in these conditions. More specific targeting of the fetal lung epithelium. Given that vectors delivered via IA injection contact the airway epithelium first, we hypothesized that there would be relatively high NP uptake in uptake in epithelial cells. However, we observed that IV injection led to better delivery of NPs to all cell types, including epithelial cells, compared with IA injection. We did observe that IA NP delivery improved with more advanced gestational age, when fetal breathing movements are more pronounced.

In an effort to optimize and specifically deliver NPs to fetal lung cells, we tested the effects of three parameters on the IV biodistribution of NPs to fetal lung: size, surface modification, and composition. To examine the effect of size, we compared large and small PLGA particles (150 nm vs. 250 nm). Previous studies have demonstrated that NP size effects accumulation in various tissues [25,26,37]. After IV administration in adult mice, when compared with larger NPs, small NPs (~120 nm) were delivered more efficiently to lung, bone marrow, specific alveolar cell populations, and hematopoietic stem and progenitor cells [21]. In our study, we found that smaller NPs (150 nm PLGA) accumulated more efficiently fetal lungs than larger NPs (250 nm PLGA). Smaller NPs were found in a greater percentage of epithelial and endothelial lung cells, but were found in a lower percentage of hematopoietic lineage cells. It has been previously demonstrated that increasing NP size can lead to greater uptake by macrophages, limiting the NPs' therapeutic potential [38]. In fetal mice, alveolar macrophages begin to differentiate at e18 [39]. However primitive macrophages originating from the fetal liver a present in the lung beginning at e12, thus the that increased uptake of larger nanoparticles by hematopoietic lineage cells may represent phagocytosis by these primitive macrophages [40].

A second parameter tested was the effect of surface modifications (PEGylation) of NPs. PEGylation of NPs improves solubility and dispersion, increases the duration of NP circulation, neutralizes NP charge, and enhances NP diffusion [41–43]. These manipulations can allow NPs to stay in circulation longer and avoid first-pass uptake by the liver and phagocytosis by local macrophages [44]. In our analysis, which was performed 3 hours after injection, PLA-PEG and PACE-PEG NPs entered endothelial cells to a greater extent than 150 nm PLGA NPs, and PLA-PEG was delivered less effectively to epithelial cells. A similar effect was also demonstrated in adult mice, where PEGylated nanocarriers were delivered more effectively to pulmonary endothelial cells and less effectively to pulmonary epithelial cells [45]. This could be a target in variants of congenital heart disease where pulmonary hypertension is expected to be a significant contributor to morbidity and mortality.

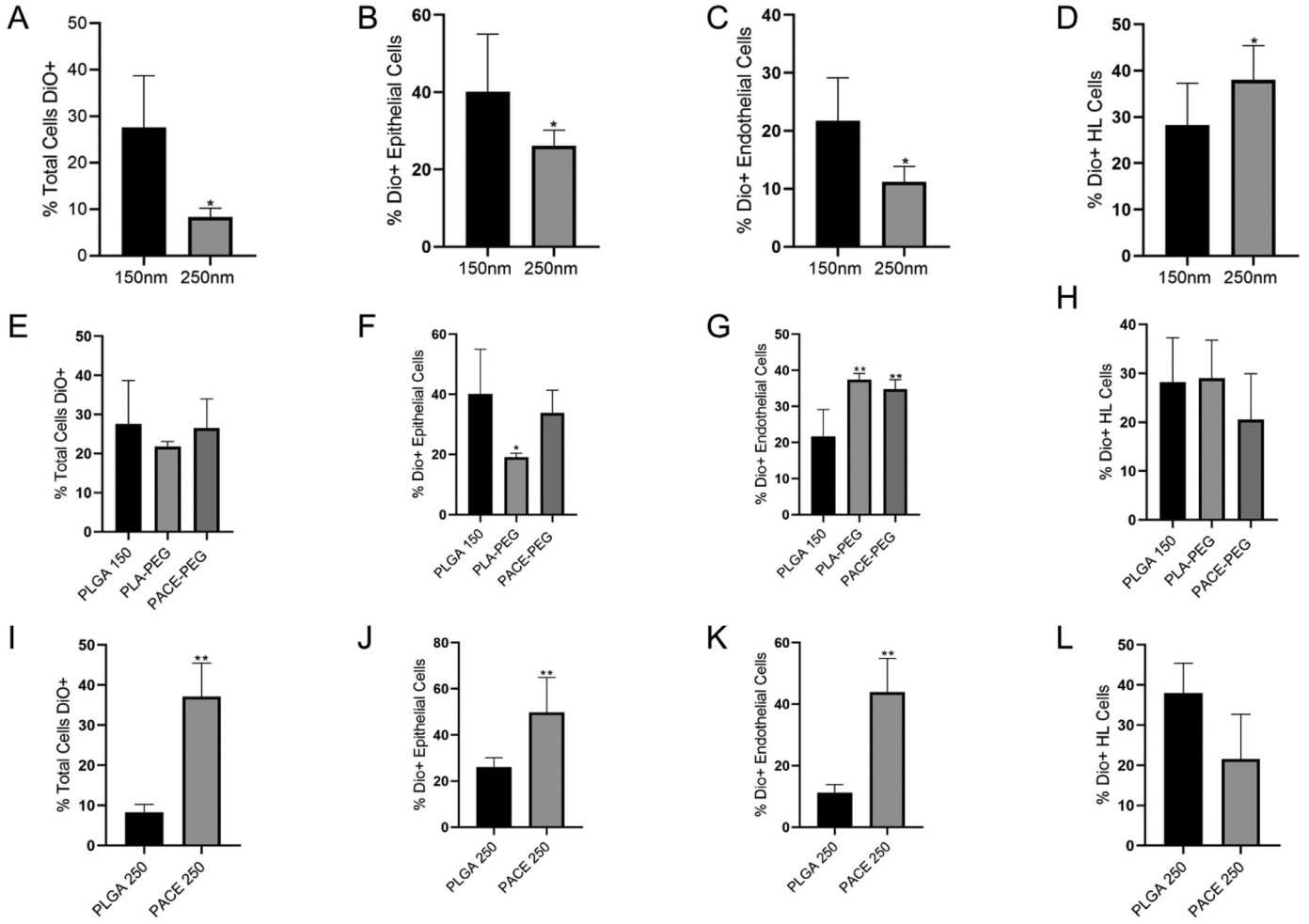

Fig. 3. NP size, polymer type and surface modification affect NP delivery to different populations of lung cells after e15 injection Bar graphs showing graph showing the percent of DiO positive cells after injection with A-D) different size NPs (unpaired student's t-test, Error bars represent S.D.) E-H) 150nm PEGylated and non-PEGylated particles (1-way ANOVA. Error bars represent S.D.) and I-L) 250 NPs with different surface charges (unpaired student's t-test, Error bars represent S.D.) total cells after e15 IV injection. 250nm NPs were considered controls. *, $p< 0.05$, **, $p<0.01$,***, $p<0.001$,****, $p< 0.000$, n=3-9.

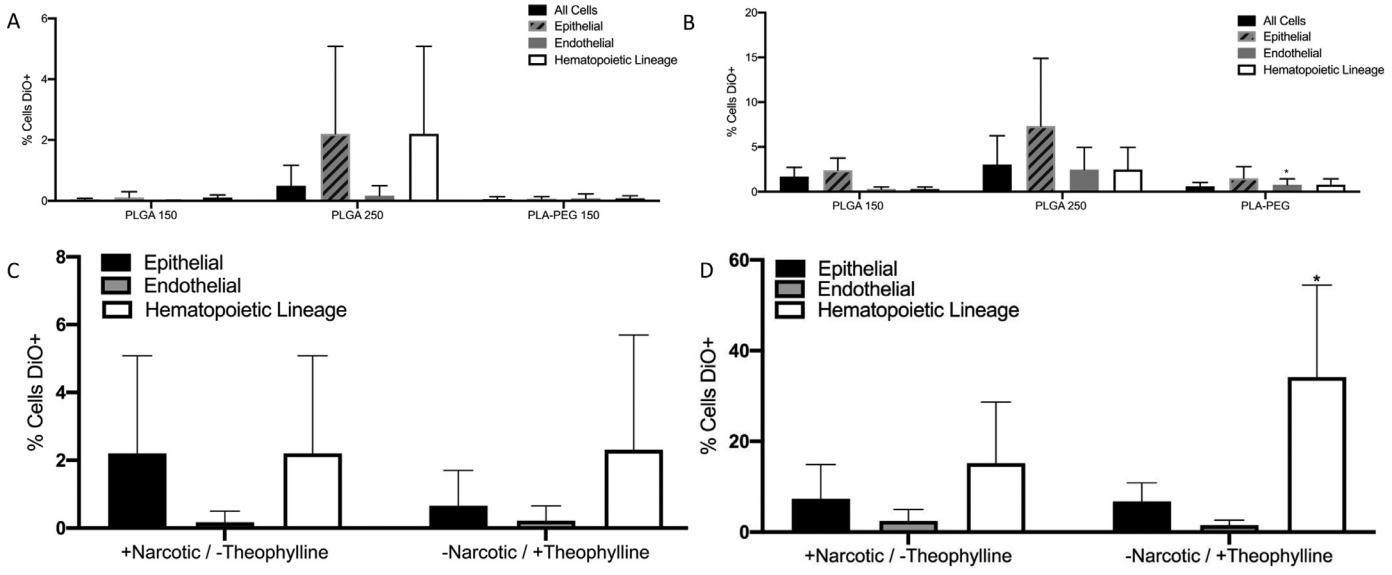

Fig. 4. IA delivery of NP to fetal lung is not improved by altering NP type or pharmacologic manipulation. **A&B)** Bar graphs of flow cytometry for % DiO NP uptake of NPs of different compositions and characteristics in all cells, epithelial, endothelial and hematopoietic cells following IA injections at **A)** e16 and **B)** e17 (1-way ANOVA. Error bars represent S.D.)**.** In an attempt to augment fetal breathing, theophylline, but no narcotic, was administered. **C&D)** Bar graphs comparing 250 nm PLGA NPs in epithelial, endothelial and hematopoietic cells by flow cytometry following **C)** e16 and **D)** e17 IA injection without theophylline and with narcotic exposure (control) and with theophylline and without narcotic. n=9-11. *, $p< 0.05$ (Unpaired student's t-test, error bars represent S.D.).

Finally, we tested the distribution of PACE NPs that were delivered more efficiently than 250 nm PLGA to both epithelial cells by two-fold and endothelial cells by nearly four-fold. Of note, PACE particles are more positively charged and have improved loading capacities for certain therapeutic agents such, as nucleic acids. The positive charge of these polymeric NPs interacts favorably with the negatively charged phospholipid cell membrane, facilitating cellular uptake [46]. PACE's improved targeting of both epithelial and endothelial cells makes it ideal for use in conditions like CDH, where both pulmonary hypoplasia and pulmonary hypertension contribute substantially to disease morbidity and mortality.

We have demonstrated previously that after IV injection, NPs accumulate most abundantly in the fetal liver, and were also detected in brain, heart, gut and kidneys in addition to fetal lung. After IA injections, NPs were delivered to the gut in as well as the lung [18]. NP accumulation was not seen in the maternal circulation or maternal liver. We have also observed that nanoparticles are present in the placenta after IV injection. The potential for off-target effects after these delivery methods makes direct intratracheal injection a seemingly ideal method for NP delivery. However, in humans as well as large and small animal models, this is not feasible until the canalicular phase of lung development [47–49]. We felt that targeting lungs at e15 through 17, during the pseudoglandular phase of lung development, when branching morphogenesis is occurring, would maximize any potential therapeutic effects.

A major limitation of IA delivery is that it requires the presence of fetal breathing movements for delivery to the lung. Previous studies have demonstrated that fetal breathing movements carry an adenoviral vector to fetal lungs [31]. However, IA delivery of NPs resulted in low levels of uptake in fetal lung and this was not improved by NP modification or pharmacologic augmentation. Theophylline has been demonstrated to improve delivery of adenoviral vectors to fetal lung; our data did not reproduce this effect for NPs, since an improvement in the delivery of NPs after theophylline exposure was only observed for hematopoietic cells at e17 [31]. We did not further characterize the hematopoietic lineage cells but presume they are resident white blood cells and macrophages in the tissue [39,40]. Another possible explanation for the poor cellular uptake of NPs in cells after IA injection is alteration to the physicochemical properties of the NP due to the protein corona formed after injection into the amniotic fluid, which is an area that warrants further investigation [50]. In the future, NPs can be delivered via fetal intra-tracheal injection in large animal models or humans which may deliver NPs more efficiently to the desired cell types.

For translation to clinical medicine, both delivery techniques would require either direct entry into the amniotic cavity or ultrasound guided umbilical artery injection, both of which come with a small but no insignificant risk of fetal loss. However, IA and IV injection minimize maternal risks, as there is no detectible NPs in maternal circulation or the liver after using either delivery methods. In addition, fetal IV injection results in more efficient delivery of therapeutic agents to the fetus, as a smaller amount of agents are needed, and the agents to not need to be transported transplacentally.

All polymers studied here have low toxicity and are biodegradable [23,51]. PLGA is the most well studied degradable polymer and is capable of sustained release, making it a popular candidate for therapeutic use [52,53]. PACE, while positively charged, has a low cationic density (to minimize toxicity), with high efficiency for nucleic acid encapsulation [16,22,54]. This study examined the biodistribution of NPs loaded with fluorescent dye, rather than therapeutic agents. Though the addition of therapeutic agents can alter the parameters studied in this article, namely surface charge and size, these can be measured and accounted for [55].

In conclusion, NPs can be delivered to fetal lung tissue following both IA and IV injection, with IV delivery being more robust but IA having the potential for more specificity to lung tissue [18]. We have demonstrated that PACE NPs target epithelial and endothelial cells better than PLGA and PLA-PEG NPs. Our hope is that optimization of uptake by the vital tissue of the fetal lung will allow correction of these tissues for devastating diseases that impair normal lung growth and function.

Funding

This work was supported by the National Institutes of Health (UG3- HL147352 to WMS and PMG). A.S.P. was supported by two NIH National Research Service Awards (NRSAs) (a T32 GM86287 training grant and an F32 HL142144 individual postdoctoral fellowship), as well as a postdoctoral research fellowship award (PIOTRO20F0) from the Cystic Fibrosis Foundation (CFF). S.J.U was supported by a Cystic Fibrosis Foundation award (STITEL17G0). S.L.A was supported by a Yale Department of Surgery Ohse Award.

Declaration of Competing Interest

Authors WMS, PMG, ASR, DHS, ASP are inventors of the following: https://patents.justia.com/patent/20200113821

Acknowledgement

The graphical abstract for this manuscript was created with BioRender.com.

Supplementary material

Supplementary material associated with this article can be found, in the online version, at doi:10.1016/j.actbio.2021.01.024.

References

[1] M.A. Coughlin, N.L. Werner, R. Gajarski, S. Gadepalli, R. Hirschl, J. Barks, M.C. Treadwell, M. Ladino-Torres, J. Kreutzman, G.B. Mychaliska, Prenatally diagnosed severe CDH: mortality an morbidity remain high, J. Pediatr. Surg. 51 (7) (2016) 1091–1095.
[2] A. Hamvas, F.S. Cole, L.M. Nogee, Genetic disorders of surfactant proteins, Neonatology 91 (4) (2007) 311–317.
[3] D.A. Stoltz, D.K. Meyerholz, M.J. Welsh, Origins of cystic fibrosis lung disease, N. Engl. J. Med. 372 (4) (2015) 351–362.
[4] S.E. Wert, J.A. Whitsett, L.M. Nogee, Genetic disorders of surfactant dysfunction, Pediatric and developmental pathology: the official journal of the Society for, Pediatr. Pathol. Paediatr.Pathol. Soc. 12 (4) (2009) 253–274.
[5] A. Vu, P.B. McCray Jr., New directions in pulmonary gene therapy, Hum. Gene Ther. 31 (17-18) (2020) 921–939.
[6] D. Alapati, W.J. Zacharias, H.A. Hartman, A.C. Rossidis, J.D. Stratigis, N.J. Ahn, B. Coons, S. Zhou, H. Li, K. Singh, J. Katzen, Y. Tomer, A.C. Chadwick, K. Musunuru, M.F. Beers, E.E. Morrisey, W.H. Peranteau, In utero gene editing for monogenic lung disease, Sci. Transl. Med. 11 (488) (2019).
[7] N. Khoshgoo, R. Visser, L. Falk, C.A. Day, D. Ameis, B.M. Iwasiow, F. Zhu, A. Ozturk, S. Basu, M. Pind, A. Fresnosa, M. Jackson, V.K. Siragam, G. Stelmack, G.G. Hicks, A.J. Halayko, R. Keijzer, MicroRNA-200b regulates distal airway development by maintaining epithelial integrity, Sci. Rep. 7 (1) (2017) 6382.
[8] S. Durrani-Kolarik, C.A. Pool, A. Gray, K.M. Heyob, M.J. Cismowski, G. Pryhuber, L.J. Lee, Z. Yang, T.E. Tipple, L.K. Rogers, miR-29b supplementation decreases expression of matrix proteins and improves alveolarization in mice exposed to maternal inflammation and neonatal hyperoxia, Am. J. Physiol. Lung Cell Mol. Physiol. 313 (2) (2017) L339–l349.
[9] N. Khoshgoo, R. Kholdebarin, P. Pereira-Terra, T.H. Mahood, L. Falk, C.A. Day, B.M. Iwasiow, F. Zhu, D. Mulhall, C. Fraser, J. Correia-Pinto, R. Keijzer, Prenatal microRNA miR-200b therapy improves nitrofen-induced pulmonary hypoplasia associated with congenital diaphragmatic hernia, Ann. Surg. 269 (5) (2019) 979–987.
[10] R. Wagner, L. Montalva, A. Zani, R. Keijzer, Basic and translational science advances in congenital diaphragmatic hernia, Semin. Perinatol. 44 (1) (2020) 151170.
[11] R. Witt, T.C. MacKenzie, W.H. Peranteau, Fetal stem cell and gene therapy, Semin. Fetal Neonatal Med. 22 (6) (2017) 410–414.
[12] W.H. Peranteau, A.W. Flake, The future of in utero gene therapy, Mol.Diagnos. Therapy 24 (2) (2020) 135–142.

[13] G. Almeida-Porada, S.N. Waddington, J.K.Y. Chan, W.H. Peranteau, T. MacKenzie, C.D. Porada, In utero gene therapy consensus statement from the IFeTIS, Mol. Ther. 27 (4) (2019) 705–707.
[14] J.H. Lee, Y. Yeo, Controlled drug release from pharmaceutical nanocarriers, Chem. Eng. Sci. 125 (2015) 75–84.
[15] O. Salata, Applications of nanoparticles in biology and medicine, J. Nanobiotechnol. 2 (1) (2004) 3.
[16] H.K. Makadia, S.J. Siegel, Poly lactic-co-glycolic acid (PLGA) as biodegradable controlled drug delivery carrier, Polymers 3 (3) (2011) 1377–1397.
[17] J. Zhou, J. Liu, C.J. Cheng, T.R. Patel, C.E. Weller, J.M. Piepmeier, Z. Jiang, W.M. Saltzman, Biodegradable poly(amine-co-ester) terpolymers for targeted gene delivery, Nat. Mater. 11 (1) (2011) 82–90.
[18] A.S. Ricciardi, R. Bahal, J.S. Farrelly, E. Quijano, A.H. Bianchi, V.L. Luks, R. Putman, F. López-Giráldez, S. Coşkun, E. Song, Y. Liu, W.C. Hsieh, D.H. Ly, D.H. Stitelman, P.M. Glazer, W.M. Saltzman, In utero nanoparticle delivery for site-specific genome editing, Nat. Commun. 9 (1) (2018) 2481.
[19] C.J. Cheng, G.T. Tietjen, J.K. Saucier-Sawyer, W.M. Saltzman, A holistic approach to targeting disease with polymeric nanoparticles, Nat. Rev. Drug Discov. 14 (4) (2015) 239–247.
[20] A. Kumari, S.K. Yadav, S.C. Yadav, Biodegradable polymeric nanoparticles based drug delivery systems, Colloids Surf. B Biointerfaces 75 (1) (2010) 1–18.
[21] H.K. Mandl, E. Quijano, H.W. Suh, E. Sparago, S. Oeck, M. Grun, P.M. Glazer, W.M. Saltzman, Optimizing biodegradable nanoparticle size for tissue-specific delivery, J. Control. Release 314 (2019) 92–101.
[22] J. Cui, A.S. Piotrowski-Daspit, J. Zhang, M. Shao, L.G. Bracaglia, T. Utsumi, Y.E. Seo, J. DiRito, E. Song, C. Wu, A. Inada, G.T. Tietjen, J.S. Pober, Y. Iwakiri, W.M. Saltzman, Poly(amine-co-ester) nanoparticles for effective Nogo-B knockdown in the liver, J. Control Release 304 (2019) 259–267.
[23] A.C. Kauffman, A.S. Piotrowski-Daspit, K.H. Nakazawa, Y. Jiang, A. Datye, W.M. Saltzman, Tunability of biodegradable poly(amine- co-ester) polymers for customized nucleic acid delivery and other biomedical applications, Biomacromolecules 19 (9) (2018) 3861–3873.
[24] M.E. Gindy, R.K. Prud'homme, Multifunctional nanoparticles for imaging, delivery and targeting in cancer therapy, Expert Opin. Drug Deliv. 6 (8) (2009) 865–878.
[25] M.A. Phillips, M.L. Gran, N.A. Peppas, Targeted nanodelivery of drugs and diagnostics, Nano Today 5 (2) (2010) 143–159.
[26] N. Hoshyar, S. Gray, H. Han, G. Bao, The effect of nanoparticle size on in vivo pharmacokinetics and cellular interaction, Nanomedicine (Lond) 11 (6) (2016) 673–692.
[27] E. Song, A. Gaudin, A.R. King, Y.E. Seo, H.W. Suh, Y. Deng, J. Cui, G.T. Tietjen, A. Huttner, W.M. Saltzman, Surface chemistry governs cellular tropism of nanoparticles in the brain, Nat. Commun. 8 (2017) 15322.
[28] Y. Deng, J.K. Saucier-Sawyer, C.J. Hoimes, J. Zhang, Y.E. Seo, J.W. Andrejecsk, W.M. Saltzman, The effect of hyperbranched polyglycerol coatings on drug delivery using degradable polymer nanoparticles, Biomaterials 35 (24) (2014) 6595–6602.
[29] M.M. Niblock, A. Perez, S. Broitman, B. Jacoby, E. Aviv, S. Gilkey, In utero development of fetal breathing movements in C57BL6 mice, Respir. Physiol. Neurobiol. 271 (2020) 103288.
[30] S.W. Glasser, M.S. Burhans, T.R. Korfhagen, C.L. Na, P.D. Sly, G.F. Ross, M. Ikegami, J.A. Whitsett, Altered stability of pulmonary surfactant in SP-C-deficient mice, Proc. Natl. Acad. Sci. U S A 98 (11) (2001) 6366–6371.
[31] S.M. Buckley, S.N. Waddington, S. Jezzard, L. Lawrence, H. Schneider, M.V. Holder, M. Themis, C. Coutelle, Factors influencing adenovirus-mediated airway transduction in fetal mice, Mol. Ther. 12 (3) (2005) 484–492.
[32] A. Bantikassegn, X. Song, K. Politi, Isolation of epithelial, endothelial, and immune cells from lungs of transgenic mice with oncogene-induced lung adenocarcinomas, Am. J. Respir. Cell Mol. Biol. 52 (4) (2015) 409–417.
[33] N.A. McNeer, K. Anandalingam, R.J. Fields, C. Caputo, S. Kopic, A. Gupta, E. Quijano, L. Polikoff, Y. Kong, R. Bahal, J.P. Geibel, P.M. Glazer, W.M. Saltzman, M.E. Egan, Nanoparticles that deliver triplex-forming peptide nucleic acid molecules correct F508del CFTR in airway epithelium, Nat. Commun. 6 (2015) 6952.
[34] J. Hanna, G.S. Hossain, J. Kocerha, The potential for microRNA therapeutics and clinical research, Front. Genet. 10 (478) (2019).
[35] R. Rupaimoole, F.J. Slack, MicroRNA therapeutics: towards a new era for the management of cancer and other diseases, Nat. Rev. Drug Discov. 16 (3) (2017) 203–222.
[36] S.M. Buckley, S.N. Waddington, S. Jezzard, A. Bergau, M. Themis, L.J. MacVinish, A.W. Cuthbert, W.H. Colledge, C. Coutelle, Intra-amniotic delivery of CFTR-expressing adenovirus does not reverse cystic fibrosis phenotype in inbred CFTR–knockout mice, Mol. Ther. 16 (5) (2008) 819–824.
[37] D.J. Lundy, K.-H. Chen, E.K.-W. Toh, P.C.-H. Hsieh, Distribution of systemically administered nanoparticles reveals a size-dependent effect immediately following cardiac Ischaemia-reperfusion injury, Sci. Rep. 6 (1) (2016) 1–10.
[38] C.D. Walkey, J.B. Olsen, H. Guo, A. Emili, W.C. Chan, Nanoparticle size and surface chemistry determine serum protein adsorption and macrophage uptake, J. Am. Chem. Soc. 134 (4) (2012) 2139–2147.
[39] M. Guilliams, I. De Kleer, S. Henri, S. Post, L. Vanhoutte, S. De Prijck, K. Deswarte, B. Malissen, H. Hammad, B.N. Lambrecht, Alveolar macrophages develop from fetal monocytes that differentiate into long-lived cells in the first week of life via GM-CSF, J. Exp. Med. 210 (10) (2013) 1977–1992.
[40] O. Lakhdari, A. Yamamura, G.E. Hernandez, K.K. Anderson, S.J. Lund, G.O. Oppong-Nonterah, H.M. Hoffman, L.S. Prince, Differential immune activation in fetal macrophage populations, Sci. Rep. 9 (1) (2019) 7677.
[41] S.K. Sahoo, J. Panyam, S. Prabha, V. Labhasetwar, Residual polyvinyl alcohol associated with poly (D,L-lactide-co-glycolide) nanoparticles affects their physical properties and cellular uptake, J. Control Release 82 (1) (2002) 105–114.
[42] J. Park, P.M. Fong, J. Lu, K.S. Russell, C.J. Booth, W.M. Saltzman, T.M. Fahmy, PEGylated PLGA nanoparticles for the improved delivery of doxorubicin, Nanomedicine 5 (4) (2009) 410–418.
[43] Y. Cu, W.M. Saltzman, Controlled surface modification with poly(ethylene)glycol enhances diffusion of PLGA nanoparticles in human cervical mucus, Mol. Pharm. 6 (1) (2009) 173–181.
[44] L. Sanchez, Y. Yi, Y. Yu, Effect of partial PEGylation on particle uptake by macrophages, Nanoscale 9 (1) (2017) 288–297.
[45] Q. Zhong, O.M. Merkel, J.J. Reineke, S.R. da Rocha, Effect of the route of administration and PEGylation of poly(amidoamine) dendrimers on their systemic and lung cellular biodistribution, Mol. Pharm. 13 (6) (2016) 1866–1878.
[46] A.Y. Kostritskii, D.A. Kondinskaia, A.M. Nesterenko, A.A. Gurtovenko, Adsorption of synthetic cationic polymers on model phospholipid membranes: insight from atomic-scale molecular dynamics simulations, Langmuir 32 (40) (2016) 10402–10414.
[47] M.S. Carlon, J. Toelen, M.M. da Cunha, D. Vidović, A. Van der Perren, S. Mayer, L. Sbragia, J. Nuyts, U. Himmelreich, Z. Debyser, J. Deprest, A novel surgical approach for intratracheal administration of bioactive agents in a fetal mouse model, J. Vis. Exp. (68) (2012).
[48] J. Deprest, E. Gratacos, K.H. Nicolaides, Fetoscopic tracheal occlusion (FETO) for severe congenital diaphragmatic hernia: evolution of a technique and preliminary results, Ultrasound Obstet. Gynecol. 24 (2) (2004) 121–126.
[49] L. Van der Veeken, F.M. Russo, L. De Catte, E. Gratacos, A. Benachi, Y. Ville, K. Nicolaides, C. Berg, G. Gardener, N. Persico, P. Bagolan, G. Ryan, M.A. Belfort, J. Deprest, Fetoscopic endoluminal tracheal occlusion and reestablishment of fetal airways for congenital diaphragmatic hernia, Gynecol. Surg. 15 (1) (2018) 9.
[50] S. Ritz, S. Schöttler, N. Kotman, G. Baier, A. Musyanovych, J. Kuharev, K. Landfester, H. Schild, O. Jahn, S. Tenzer, V. Mailänder, Protein corona of nanoparticles: distinct proteins regulate the cellular uptake, Biomacromolecules 16 (4) (2015) 1311–1321.
[51] S.S. Panchal, D.V. Vasava, Biodegradable polymeric materials: synthetic approach, ACS Omega 5 (9) (2020) 4370–4379.
[52] D. Essa, P.P.D. Kondiah, Y.E. Choonara, V. Pillay, The design of poly(lactide-co-glycolide) nanocarriers for medical applications, Front. Bioeng. Biotechnol. 8 (2020) 48.
[53] R.J. Fields, E. Quijano, N.A. McNeer, C. Caputo, R. Bahal, K. Anandalingam, M.E. Egan, P.M. Glazer, W.M. Saltzman, Modified poly(lactic-co-glycolic acid) nanoparticles for enhanced cellular uptake and gene editing in the lung, Adv. Healthc. Mater. 4 (3) (2015) 361–366.
[54] F. Danhier, E. Ansorena, J.M. Silva, R. Coco, A.Le Breton, V. Preat, PLGA-based nanoparticles: an overview of biomedical applications, J. Control Release 161 (2) (2012) 505–522.
[55] A.S. Piotrowski-Daspit, A.C. Kauffman, L.G. Bracaglia, W.M. Saltzman, Polymeric vehicles for nucleic acid delivery, Adv. Drug. Deliv. Rev. 156 (2020) 119–132.